THE JOURNAL OF BIOLOGICAL CHEMISTRY VOL. 286, NO. 7, pp. 5375–5382, February 18, 2011

Rab27a Negatively Regulates Phagocytosis by Prolongation of the Actin-coating Stage around Phagosomes*[S]

Received for publication, August 3, 2010, and in revised form, December 9, 2010 Published, JBC Papers in Press, December 18, 2010, DOI 10.1074/jbc.M110.171702

Kunio Yokoyama[‡], Hiroaki Kaji[§], Jinsong He[¶], Chisato Tanaka[§], Ryoichi Hazama[§‖], Takashi Kamigaki[‡], Yonson Ku[**], Kaoru Tohyama[‡‡], and Yumi Tohyama[§1]

From the [‡]Division of Gastroenterological Surgery, [**]Division of Hepato-Biliary-Pancreatic Surgery, and [‖]Division of Biochemistry, Department of Molecular and Cellular Biology, Kobe University Graduate School of Medicine, Kobe 650-0017, Japan, the [§]Division of Biochemistry and [¶]Department of Pharmaceutical Health Care, Faculty of Pharmaceutical Sciences, Himeji Dokkyo University, Himeji 670-8524, Japan, and the [‡‡]Department of Laboratory Medicine, Kawasaki Medical School, Kurashiki 701-0192, Japan

Rab27a, a Rab family small GTPase, is involved in the exocytosis of secretory granules in melanocytes and cytotoxic T-cells. Rab27a mutations cause type 2 Griscelli syndrome, which is characterized by immunodeficiency, including uncontrolled macrophage activation known as hemophagocytic syndrome. However, the role of Rab27a in phagocytosis remains elusive. Here, using macrophage-like differentiated HL-60 cells and C3bi-opsonized zymosan as a pathogen-phagocyte model, we show that Rab27a negatively regulates complement-mediated phagocytic activity in association with F-actin remodeling. We found that transfection of Rab27a shRNA into HL-60 cells enhances complement-mediated phagocytosis. To clarify the mechanisms underlying the elevated phagocytosis in Rab27a knockdown cells, we analyzed the process of phagosome formation focusing on F-actin dynamics: F-actin assembly, followed by F-actin extension around the particles and the subsequent degradation of F-actin, leading to internalization of the particles enclosed in phagosomes. Microscopic analysis revealed that these actin-related processes, including F-actin coating and F-actin degradation, proceed more rapidly in Rab27a knockdown cells than in control HL-60 cells. Both elevated phagocytosis and accelerated F-actin remodeling were restored by expression of rescue-Rab27a and Rab27a-Q78L (GTP-bound form), but not by Rab27a-T23N (GDP-bound form). Furthermore, an increased accumulation of Coronin 1A surrounding F-actin coats was observed in Rab27a knockdown cells, suggesting that the function of Coronin 1A is related to the regulation of the F-actin coating. Our findings demonstrate that Rab27a plays a direct regulatory role in the nascent process of phagocytosis by prolongation of the stage of actin coating via suppression of Coronin 1A. This study may contribute to an explanation of the underlying mechanisms of excessive phagocytosis observed in Griscelli syndrome.

Rab27a is a member of the Rab family of small GTPase proteins. The Rab GTPases control almost all membrane trafficking processes, including vesicle budding, docking and fusion to acceptor membranes, and exosome release (1, 2). Rab27a is involved in the exocytosis of secretory granules in melanocytes and cytotoxic T lymphocytes. Mutations in Rab27a cause type 2 Griscelli syndrome, which is characterized not only by pigment dilution but also by defects in cytotoxic granule transport and by macrophage activation syndrome (known as hemophagocytic syndrome) (3–5).

Efficient phagocytosis of pathogens is crucial for an immune response, and macrophages are professional phagocytes as well as neutrophils and dendritic cells. Macrophages express a variety of phagocytic receptors, such as the Fcγ receptor, C-type lectin receptors, and complement receptor 3, also known as integrin αMβ2, which recognizes activated complement C3bi. Phagocytosis is triggered by an association between ligands on the surface of pathogens and receptors on the membrane of phagocytes. Receptor clustering at the attachment site generates phagocytic signaling that leads to local actin polymerization and to phagosome formation. First, transient assembly of F-actin occurs beneath the target particles. Subsequently, actin coating begins at the nascent phagocytic cup and extends around the phagosome (6). Once the wrapping is completed, the actin coating rapidly disappears, and the particles are then completely internalized (7). The rapid collapse of the assembled F-actin is regulated by the level of phosphatidylinositol 4,5-bisphosphate (PIP_2),[2] which is determined by the balance between the synthesis of PIP_2 by phosphatidylinositol-4-phosphate 5-kinase and its degradation by phospholipase C (8, 9).

Rab27a has been reported to regulate phagosomal pH during phagocytosis via mediation of the fusion of phagosomes with NOX2-positive vesicles (10). The synaptotagmin-like family proteins and the myosin family motor protein myosin Va are well characterized downstream effectors of Rab27a in melanocytes, but their role in Rab27a function in macrophages has not yet been demonstrated (11–14). Coronins are actin-binding proteins that are involved in phagocytosis (15, 16), chemotaxis, and lamellipodial formation, and Coronin 1

* This work was supported in part by KAKENHI and a grant-in-aid for scientific research (C) from the Japan Society for the Promotion of Sciences (to Y. T. and K. T.).

[S] The on-line version of this article (available at http://www.jbc.org) contains supplemental Figs. S1 and S2.

[1] To whom correspondence should be addressed: Div. of Biochemistry, Faculty of Pharmaceutical Sciences, Himeji Dokkyo University, Himeji 670-8524, Japan. Tel.: 81-79-223-6809; Fax: 81-79-285-0352; E-mail: ytohyama@himeji-du.ac.jp.

[2] The abbreviations used are: PIP_2, phosphatidylinositol 4,5-bisphosphate; pAb, polyclonal antibody.

is believed to be a key regulator of actin disassembly whose activity is regulated by PIP_2 (17).

In this study, we investigated whether Rab27a is directly involved in the process of phagocytosis in the complement-mediated pathway. Our results show that Rab27a negatively regulates phagocytosis by prolongation of the actin-coating stage via suppression of Coronin 1A accumulation at F-actin coats.

EXPERIMENTAL PROCEDURES

Reagents and Antibodies—Zymosan A, Alexa Fluor 594-conjugated zymosan A, Alexa Fluor 488-conjugated zymosan A, Alexa Fluor 594-conjugated phalloidin, Alexa Fluor 488-conjugated phalloidin, and a ViraPower lentiviral directional TOPO expression kit were purchased from Invitrogen. RPMI 1640 medium and hygromycin were from Wako (Osaka, Japan), and puromycin was purchased from Sigma. Penicillin/streptomycin mixed solution was from Nacalai Tesque (Kyoto, Japan), and Polybrene was purchased from Millipore (Bedford, MA). Rabbit anti-human Rab27a polyclonal antibody (pAb), mouse anti-FLAG monoclonal antibody M2 (mAb), and Cy3-conjugated mouse anti-FLAG mAb M2 were purchased from Sigma. Mouse anti-human CD11b (C3bi receptor) mAb for flow cytometry was purchased from DAKO (Glostrup, Denmark). Mouse anti-human LAMP-1 (lysosome-associated membrane protein 1) mAb was from BD Biosciences, mouse anti-human LAMP-1 (H4A3) mAb was from Santa Cruz Biotechnology (Santa Cruz, CA), and mouse anti-human Coronin 1A mAb was purchased from Abcam (Cambridge, UK).

Cells and Cell Culture—A human leukemia cell line (HL-60) was maintained in RPMI 1640 medium supplemented with 8% heat-inactivated FCS, 100 units/ml penicillin, and 100 μg/ml streptomycin in 5% CO_2-humidified air at 37 °C. The cells were induced to undergo differentiation to macrophages by seeding them on dishes at a concentration of 2×10^6 cells/100-mm dish or 1×10^5 cells/35-mm glass-based dish (glass diameter, 12 mm) in the presence of 10^{-7} M 1,25-dihydroxycholecalciferol (vitamin D_3) and 10 ng/ml 12-*O*-tetradecanoylphorbol-13-acetate and incubating for 3 days. Cell differentiation was confirmed morphologically by evaluating complement receptor 3 by flow cytometry. The study dealing with the blood from healthy volunteers had been approved by the ethical committee of Himeji Dokkyo University, and the samples were handled after informed consent. Human monocytes were collected using the magnetic cell sorting system and microbeads conjugated with monoclonal mouse anti-human CD14 antibody (Miltenyi Biotec, Bergisch Gladbach, Germany). Briefly, peripheral blood mononuclear cells of healthy blood donors were isolated by density gradient centrifugation using Ficoll-Paque (Pharmacia Biotech AB, Uppsala, Sweden). CD14-expressing cells were positively separated by the magnetic cell sorting system according to the protocol provided by the manufacturer.

Plasmids and Transfection—To inhibit *Rab27A* gene expression, a vector for shRNA incorporated in pLKO.1-puro (Sigma, MISSION shRNA code TRCN 0000005294) was transfected into HL-60 cells by the lentiviral system, and positive clones were selected with 1 μg/ml puromycin. To support the knockdown effects of *Rab27A* shRNA, we constructed FLAG-rescue-Rab27a, FLAG-rescue-Rab27a-Q78L, and FLAG-rescue-Rab27a-T23N expression vectors. Complementary DNA encoding human Rab27a was isolated and amplified from the cDNA library of a human megakaryoblastic leukemia cell line, CMK, with the following primer pair using Micro-FastTrack (Invitrogen): 1–26 sense primer, 5′-ATGTCTGATGGAGATTATGATTACCT-3′; and 640–666 antisense primer, 5′-TCAACAGCCACATGCCCCTTTCTCCTT-3′. The second amplification reaction was performed with sense primer containing the BamHI restriction site and FLAG sequence and antisense primer containing the EcoRI site. The amplified products were cloned into pcDNA4/TO (Invitrogen) and then subcloned into the pLenti6/V5-D-TOPO vector (Invitrogen). FLAG-Rab27a-Q78L was constructed by two-step overlap extension PCR. To amplify two fragments, we used 64–89 sense primer (5′-AAGAACAGTGTACTTTACCAATATAC-3′) and 49–87 antisense primer (5′-ATATTGGTAAAGTACACTGTTCTTCCCTACACCAGAGTC-3′), presenting mutation 68C→A, in addition to the previous primer set. Two fragments were combined by PCR. Similarly, Rab27a-T23N was also constructed by two-step overlap extension PCR using 229–255 sense primer (5′-AAGAACAGTGTACTTTACCAATATAC-3′) and 214–252 antisense primer (5′-TAA GCTACGAAACCTCTCCAGCCCTGCTGTGTCCCATAAC-3′), presenting mutation 233A→T, in addition to the previous primer set. These constructs were verified using an Applied Biosystems 3130 genetic analyzer. FLAG-rescue-Rab27a was introduced into Rab27A shRNA/HL cells by electroporation or the lentiviral system, and positive clones were selected with 5 μg/ml blasticidin for pLenti6/V5-D-TOPO. The effects of shRNA on expression of Rab27a and FLAG-rescue-Rab27a were confirmed by immunoblot analysis with mouse anti-FLAG mAb M2 and rabbit anti-human Rab27a pAb. For transient expression of FLAG-rescue-Rab27a, FLAG-rescue-Rab27a-Q78L, and FLAG-rescue-Rab27a-T23N, these vectors were transfected into Rab27a shRNA/HL cells by the lentiviral system and induced to undergo differentiation to macrophages as described above.

Phagocytosis Assay—A complement-mediated phagocytosis assay was performed as described previously (18). Briefly, to opsonize zymosan with C3bi, the complement activation cascade in serum was utilized. Zymosan A was incubated in 50% human serum at 37 °C for 30 min and then washed with PBS twice at 4 °C. C3bi-opsonized or non-opsonized zymosan was added to macrophage-like differentiated HL-60 cells (ratio of cells to zymosan particles of 1:10) and incubated for the indicated times at 37 °C. For quantitative analysis of the phagocytosis assay by flow cytometry, Alexa Fluor 594-conjugated zymosan A was used similarly as described above and analyzed by flow cytometry (FACSCalibur, BD Biosciences). Macrophage-like differentiated HL-60 cells were also pretreated with 1 μM jasplakinolide (Enzo Life Sciences) for 2 h before quantitative analysis of the phagocytosis assay. To determine whether zymosan particles exist inside or outside the cells, Alexa Fluor 488-conjugated zymosan A was used, and a phago-

cytosis assay was performed as described above; the cells were then analyzed by fluorescence microscopy before and after treatment with 0.2% trypan blue in PBS.

Immunofluorescence Microscopic Analysis—The cells were washed three times with PBS after the phagocytosis assay and fixed with 3.3% paraformaldehyde for 15 min. Cells were washed twice with PBS containing 1 mM $MgCl_2$ and 0.1% BSA (staining buffer), permeabilized with 0.2% Triton X-100 in staining buffer for 3 min, and blocked with PBS containing 1 mM $MgCl_2$ and 5% BSA for 30 min. To assess the distribution of Rab27a, cells were incubated with rabbit anti-human Rab27a pAb for 1 h and washed three times with staining buffer. Then, cells were incubated with Alexa Fluor 488-conjugated secondary goat anti-rabbit IgG pAb (Invitrogen) for 30 min. To assess the distribution of Coronin 1A and F-actin, a phagocytosis assay was started as described above, and the cells were treated with C3bi-zymosan for 10 min at 37 °C. After washing twice to remove unbound C3bi-zymosan particles, the treated cells were reincubated for the indicated times at 37 °C and then fixed and permeabilized. Cells were incubated with mouse anti-Coronin 1A mAb for 1 h and then with Alexa Fluor 594-conjugated secondary goat anti-mouse IgG pAb (Invitrogen) and Alexa Fluor 488-conjugated phalloidin. To analyze the effects of transient expression of FLAG-rescue-Rab27a, FLAG-rescue-Rab27aQ78L, and FLAG-rescue-Rab27aT23N on phagocytic activity, cells were incubated with mouse anti-Coronin 1A mAb for 1 h and then with Alexa Fluor 488-conjugated secondary goat anti-mouse IgG pAb (Invitrogen) and mouse anti-FLAG M2-Cy3 mAb. Stained cells were washed three times with staining buffer and observed with a confocal laser-scanning microscope (LSM 510 META, Carl Zeiss, Oberkochen, Germany).

Phagosome-Lysosome Fusion Assay—To study the degree of phagosome-lysosome fusion, C3bi-opsonized Alexa Flour 488-conjugated zymosan A was added to macrophage-like differentiated HL-60 cells (ratio of cells to zymosan particles of 1:10), and the cells were incubated for 10 min, washed three time with PBS, and further incubated for the indicated times at 37 °C. After incubation, cells were washed three times with PBS and then fixed and permeabilized. Cells were incubated with anti-LAMP-1 antibodies and observed with a confocal laser-scanning microscope. Phagosomes surrounded by LAMP-1 were counted as fused lysosomes. More than 50 zymosan particles were counted, and the ratio of fused zymosan particles to attached ones was calculated.

Immunoblot Analysis—Cells were lysed with lysis buffer (1% Triton X-100, 50 mM Tris-HCl (pH 7.2), 100 mM NaCl, 5 mM EDTA, and 1 mM phenylmethylsulfonyl fluoride). Proteins were separated by SDS-PAGE and transferred to a polyvinylidene difluoride membrane (Millipore). The membrane was blocked with 5% skim milk in T-TBS (0.1% Tween 20, 25 mM Tris-HCl (pH 8.0), and 150 mM NaCl) for 60 min at room temperature and then incubated with the appropriate antibodies. The membrane was washed three times with T-TBS and incubated with horseradish peroxidase-conjugated goat anti-rabbit or anti-mouse antibodies for 30 min, and specific proteins were detected using an enhanced chemiluminescence immunoblotting system and a LuminoImage analyzer (LAS-3000, Fuji Photo Film, Tokyo, Japan).

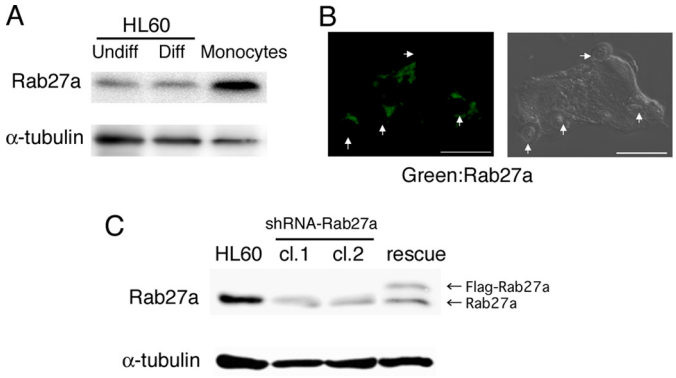

FIGURE 1. **Rab27a is expressed in human phagocytic cells.** *A*, Rab27a expression in HL-60 cells, macrophage-like differentiated (*Diff*) HL-60 cells treated with vitamin D_3 and 12-*O*-tetradecanoylphorbol-13-acetate for 3 days, and peripheral blood-derived monocytes were analyzed by immunoblotting with antibodies against human Rab27a and α-tubulin as a loading control. *B*, a phagocytosis assay was performed using macrophage-like differentiated HL-60 cells and C3bi-zymosan for 30 min as described under "Experimental Procedures." Distribution of Rab27a was analyzed by staining with anti-Rab27a antibodies (*left*) and a differential interference contrast image (*right*). *Scale bar* = 5 μm. *Arrowheads* show C3bi-zymosan particles. *C*, decreased expression of Rab27a by Rab27a shRNA transfer into HL-60 cells (clones 1 (*cl.1*) and 2 (*cl.2*)) and its recovery by FLAG-rescue-Rab27a into Rab27a knockdown cells by immunoblotting with antibodies against human Rab27a and α-tubulin as a loading control.

Statistical Analysis—In some experiments, statistical significance was determined by Student's *t* test.

RESULTS

To investigate the role of Rab27a in phagocytic cells, we first analyzed the expression level of Rab27a in HL-60 cells, macrophage-like differentiated HL-60 cells (18, 19), and human peripheral blood-derived monocytes by immunoblot analysis. Rab27a was clearly detected in all of these cells (Fig. 1*A*). We then examined the subcellular localization of Rab27a during complement-mediated phagocytosis using macrophage-like differentiated HL-60 cells and serum-opsonized zymosan (C3bi-zymosan) as described previously (18). After the onset of complement-mediated phagocytosis, Rab27a was accumulated around phagosomes with a vesicular structure (Fig. 1*B*). These results suggest that Rab27a is involved in the nascent phase of complement-mediated phagocytosis. To further investigate the role of Rab27a in phagocytosis, Rab27a knockdown HL-60 clones were established by transfecting Rab27a previously into HL-60 cells using a lentiviral system (Rab27a shRNA/HL). Transfection of Rab27a shRNA successfully reduced the expression of endogenous Rab27a protein in HL-60 cells (clone 1 by an 80% decrease; clone 2 by an 82% decrease), and transfection of FLAG-tagged Rab27a, which was designed to be resistant to this shRNA, into Rab27a shRNA/HL restored the expression of Rab27a (rescue-Rab27a shRNA/HL) (Fig. 1*C*). Flow cytometric analysis showed that the level of cell-surface expression of complement receptor 3 after macrophage-like differentiation induction was unchanged among parental HL-60 cells and Rab27a shRNA/HL and rescue-Rab27a shRNA/HL clones (data not shown).

We next examined the effects of Rab27a knockdown on phagocytic activity using fluorescence-labeled zymosan as

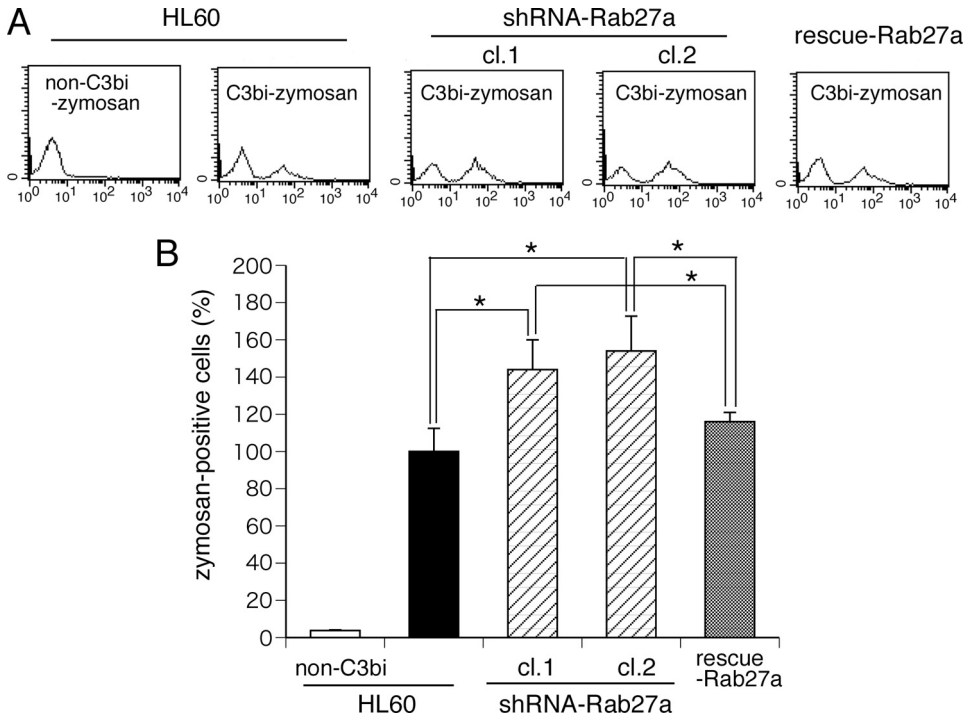

FIGURE 2. **Complement-mediated phagocytosis is enhanced in Rab27a knockdown cells.** A phagocytosis assay was performed using HL-60 cells, Rab27a shRNA/HL cells (clones 1 (*cl.1*) and 2 (*cl.2*)), and FLAG-rescue-Rab27a/Rab27a shRNA/HL cells. The cells that incorporated C3bi-labeled Alexa Fluor 594-conjugated zymosan shifted to the right by flow cytometry. *A*, representative data are shown. *B*, results of the phagocytosis assay are shown in histograms. The data are means ± S.D. from four independent experiments. *, statistically significant difference ($p < 0.05$).

described previously (18). As shown in Fig. 2 (*A* and *B*), transfection of Rab27a shRNA promoted the phagocytosis of C3bi-opsonized zymosan, and this elevated phagocytic activity was reversed by transfection of rescue-Rab27a. These results indicate that Rab27a negatively regulates complement-mediated phagocytosis in macrophage-like differentiated HL-60 cells. To clarify the stage during which Rab27a regulates phagocytic activity, a fluorescence quenching assay using trypan blue, which can distinguish between zymosan particles inside and outside the cell, was performed. We first analyzed the kinetics in uptake of complement-opsonized zymosan at 5 min after the onset of phagocytosis before the quenching assay and confirmed that, before internalization, the uptake of zymosan was equal to that of parental HL-60 cells. The percentage of zymosan particles ingested into the cell in Rab27a knockdown cells was ~50% higher than that in parental HL-60 cells at 30 min after the onset of phagocytosis (percentage of engulfed zymosan, 33.7 ± 9.7 in HL-60 cells and 56.4 ± 10.0 in Rab27a knockdown cells). These results show that the increased phagocytosis of Rab27a knockdown cells was not due to increased binding of C3bi-zymosan to complement receptor 3 but, instead, was due to rapid internalization of captured zymosan particles.

To clarify the mechanisms by which Rab27a knockdown promotes the engulfment of attached particles, actin remodeling was monitored during the early stage of complement-mediated phagocytosis in parental and Rab27a knockdown HL-60 cells using fluorescence microscopy. Ten min after the onset of complement-mediated phagocytosis, non-attached C3bi-zymosan particles were removed, and the cells were incubated for the indicated times. Immediately after washing, actin was detected mainly as an accumulation beneath the attached particles (Fig. 3*A*, *panel a*). Ten or 20 min after washing, there was an increase in the number of F-actin-coated structures such as hemispheric actin cups (Fig. 3*A*, *panel b*) and spherical actin coats (*panel c*) around the zymosan particles. Occasionally, the spherical actin coat appeared punctate (Fig. 3*A*, *panel d*). Actin filaments were not detected around phagosomes that were completely ingested (Fig. 3*A*, *panel e*), in accordance with previous reports regarding Fcγ receptor-mediated phagocytosis (7). To evaluate the effect of Rab27a knockdown on actin remodeling during the process of engulfment, F-actin structures around the zymosan particles were classified into five categories based on the temporal phases of actin remodeling (Fig. 3*A*, *panels a–e*). As shown in Fig. 3*B*, in Rab27a shRNA/HL cells, the process of actin reorganization required to complete phagosome formation occurred more quickly than in parental HL-60 cells. In other words, the actin-coating process was shortened in Rab27a knockdown cells, and rapid degradation of F-actin resulted in effective internalization of zymosan particles. In addition, the ratio of punctate actin was higher in Rab27a shRNA/HL cells (Fig. 3*B*). These results suggest that the acceleration of F-actin remodeling leads to a marked increase in phagocytosis in Rab27a knockdown cells.

Because actin dynamics also has an important role in phagosome-lysosome fusion during the phagocytic process, the effect of Rab27a knockdown on the velocity of phagosome-lysosome fusion was scored using LAMP-1 as a lysosomal membrane marker (Fig. 4). The ratio of fused to non-fused phagosomes with lysosomes in Rab27a knockdown cells was significantly higher than that in parental HL-60 cells at 1 h

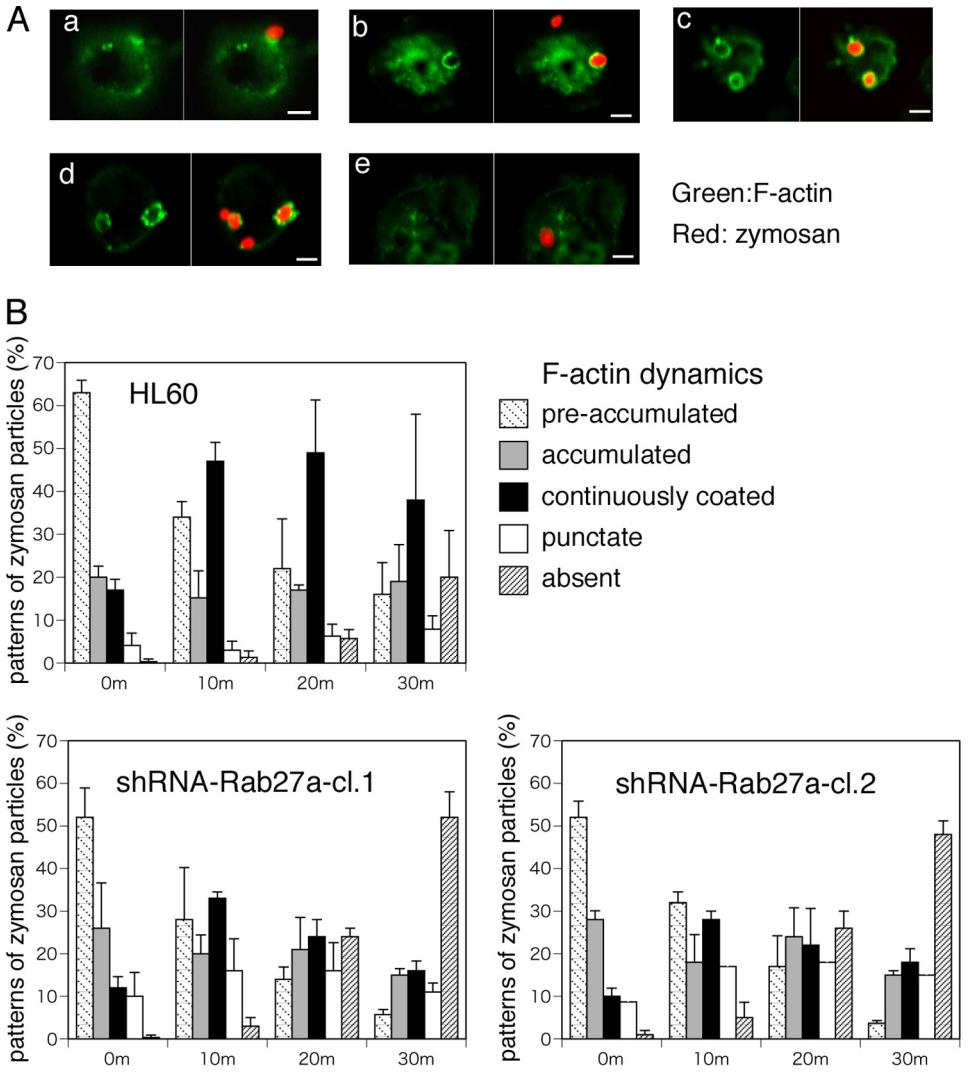

FIGURE 3. **Acceleration of actin remodeling leads to increased phagocytosis in Rab27a knockdown cells.** A phagocytosis assay was performed using C3bi-labeled Alexa Fluor 594-conjugated zymosan for 10 min. Treated cells were washed with PBS and further incubated for the indicated times. *A*, cells were stained with Alexa Fluor 488-conjugated phalloidin and classified into actin accumulation beneath the attached particles (*panel a*), F-actin-coating structure around the zymosan particles such as hemisphere actin cups (*panel b*), spherical actin coating (*panel c*), actin coating shredded in pieces (*panel d*), and disappearance of actin filaments around phagosomes (*panel e*). *Scale bars* = 5 μm. *B*, patterns of zymosan particles in the process of phagocytosis in HL-60 and Rab27a shRNA/HL cells (clones 1 (*cl.1*) and 2 (*cl.2*)). Each zymosan particle was classified into five stages according to F-actin dynamics as indicated. More than 100 zymosan particles were classified into five stages, and the proportion of the stages was changed with the indicated time course up to 30 min. The data are means ± S.D. from three independent experiments.

after washing, but the ratio of fusion in Rab27a knockdown cells was equal to that in parental HL-60 cells at 2 h after washing (Fig. 4). These results raise the possibility that the prompt fusion observed in Rab27a knockdown cells at 1 h reflects rapid actin remodeling; however, so far as we examined the LAMP-1-positive phagosomes, there were no significant differences in the ratio of fused phagosomes at 2 h after washing.

To elucidate the molecular mechanism by which actin coating of phagosomes is prolonged by Rab27a, we explored the role of signaling molecule(s) downstream of Rab27a during complement-mediated phagocytosis. Actin dynamics is regulated by actin-binding proteins, which are temporally and spatially regulated by PIP_2. We focused our analysis on Coronin 1A because Coronin 1A is reported to bind both PIP_2 and actin filaments (17) and is involved in phagocytosis in HL-60 cells (16). We first determined the expression level of Coronin 1A in parental and Rab27a knockdown HL-60 cells by immunoblot analysis (Fig. 5*A*). We next assessed the dynamics of intracellular localization of Coronin 1A concurrently with F-actin remodeling. As shown in Fig. 5*B*, 10 min after washing, zymosan particles either were surrounded only by F-actin (*panel a*) or were surrounded in the linear form by both Coronin 1A and F-actin (*panel b*). Thirty min after washing, punctate colocalization of Coronin 1A and F-actin around particles was increased (*panel c*), and phagosomes were formed inside the cells, and at that time, neither Coronin 1A nor F-actin surrounded zymosan particles (*panel d*). These results suggest that actin coating occurs during the process of phagosome formation, which is followed by Coronin 1A accumulation, and, that coated F-actin disappears during the step of particle engulfment. To evaluate the effect of Rab27a knockdown on the interaction between Coronin 1A and F-actin remodeling, the colocalization patterns of Coronin 1A and F-actin around

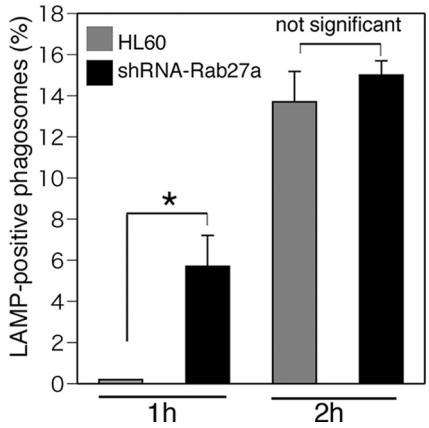

FIGURE 4. **Effects of Rab27a on lysosomal fusion with phagosomes.** Phagocytosis assay was performed using C3bi-labeled Alexa Fluor 594-conjugated zymosan for 10 min in HL-60 and Rab27a shRNA/HL cells (clone 1). Treated cells were washed with PBS and further incubated for the indicated times. Fusion of lysosomes with phagosomes was determined by staining with anti-LAMP-1 antibodies. More than 50 zymosan particles were counted, and the ratio of fused zymosan particles to attached ones was calculated. The data are means ± S.D. from three independent experiments. *, statistically significant difference ($p < 0.05$).

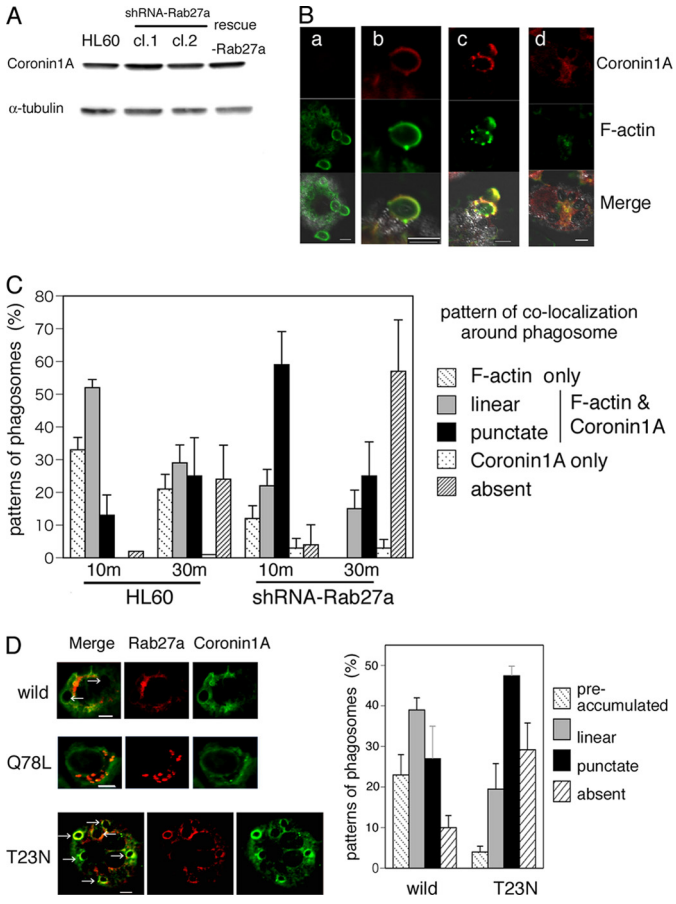

FIGURE 5. **Rab27a retains the actin-coating process by regulating Coronin 1A movement into phagosomes during complement-mediated phagocytosis.** *A*, expression of Coronin 1A in HL-60 cells, Rab27a shRNA/HL cells (clones 1 (*cl.1*) and 2 (*cl.2*)), and FLAG-rescue-Rab27a/Rab27a shRNA cells by immunoblot analysis with antibodies against human Coronin 1A and α-tubulin as a loading control. *B*, distribution of Coronin 1A together with F-actin remodeling in the process of complement-mediated phagocytosis. Ten min after washing, zymosan particles were surrounded only by F-actin (*panel a*), and zymosan particles were surrounded in the linear form by both Coronin 1A and F-actin (*panel b*). Thirty min after washing, a dotted pattern of colocalization of Coronin 1A and F-actin around particles was seen (*panel c*). Phagosomes were formed inside the cells, and zymosan particles were not surrounded with Coronin 1A or F-actin (*panel d*). *Scale bars* = 5 μm. *C*, patterns of colocalization of Coronin 1A and F-actin around zymosan particles in the process of complement-mediated phagocytosis were counted in HL-60 and Rab27a shRNA/HL cells (clone 1). Patterns of colocalization of Coronin 1A and F-actin around zymosan particles were classified into five stages as indicated. More than 100 zymosan particles were classified into five stages, and the proportion of the stages was changed with the indicated time course up to 30 min. The data are means ± S.D. from three independent experiments. *D*, costaining of Coronin 1A (*green fluorescence*) and transiently expressed FLAG-tagged Rab27a visualized by Cy3-conjugated anti-FLAG antibody (*red fluorescence*) shown as wild-type Rab27a, Rab27a-Q78L (GTP-bound form), or Rab27a-T23N (GDP-bound form) in Rab27a shRNA/HL cells (clone 1) after phagocytosis assay for 30 min (*left*). *Scale bars* = 10 μm. The histograms indicate that the accumulation of Coronin 1A around phagosomes is promoted in Rab27a-T23N-expressing cells (*right*). Patterns of Coronin 1A accumulation around phagosomes were classified into four stages as indicated. More than 50 phagosomes were evaluated per assay. The data are means ± S.D. from three independent experiments.

zymosan particles were classified into five stages (Fig. 5*C*). Rab27a knockdown significantly increased the punctate pattern of colocalization of Coronin 1A and F-actin around phagosomes at 10 min after washing, and particle engulfment was markedly accelerated at 30 min after washing (Fig. 5*C*). These results suggest that rapid accumulation of Coronin 1A in Rab27a knockdown cells promotes rapid F-actin remodeling, which leads to accelerated phagocytosis.

Finally, to examine the effects of Rab27a GTPase activity on both phagosome formation and Coronin 1A accumulation, FLAG-rescue-Rab27a (wild-type form), FLAG-Rab27a-T23N (GDP-bound form), or FLAG-Rab27a-Q78L (GTP-bound form) was transiently expressed in Rab27a knockdown cells. As shown in Fig. 5*D* (*left*), phagocytosis was attenuated in wild-type Rab27a- and Rab27a-Q78L-expressing cells (number of zymosan particles, 4.2 ± 1.3 per Rab27a knockdown cell, 2.5 ± 1.8 per wild-type Rab27a-expressing cell, and 0.79 ± 1.3 per Rab27a-Q78L-expressing cell). In contrast, phagocytosis occurred normally or was even enhanced in Rab27a-T23N-expressing cells (6.7 ± 1.5 per Rab27a-T23N-expressing cell). The histograms indicate that the accumulation of Coronin 1A around phagosomes is promoted in Rab27a-T23N-expressing cells (Fig. 5*D* (*right*) and supplemental Fig. S1). In addition, we confirmed that transfer of Coronin 1A shRNA prolongs the actin-coating stage in the process of phagocytosis (supplemental Fig. S2). These results suggest that the expression of GTP-bound Rab27a is essential for negative regulation of phagocytosis and that conversion to GDP-bound form promotes Coronin 1A-related actin disassembly.

DISCUSSION

In this study, we aimed to clarify the role of Rab27a in the process of phagocytosis and showed that Rab27a negatively regulates phagocytosis due to prolongation of the stage of actin coating via suppression of Coronin 1A. Although mutations in Rab27a cause type 2 Griscelli syndrome associated with hemophagocytic syndrome, the direct role of Rab27a in macrophage function has not been clarified yet. Amigorena and co-workers (10) demonstrated that Rab27a also contributes to microbial antigen cross-presentation by dendritic cells

and that the recruitment of Rab27a to phagosomes regulates phagosomal pH, rescues peptides against excessive degradation in acidic lysosomes, and allows efficient cross-presentation. In addition to these previous concepts, our present data demonstrate that Rab27a plays a direct regulatory role in the process of macrophage phagocytosis. Collectively, Rab27a might play a regulating role in the phagocytic process: 1) degradation in phagolysosomes and 2) internalization of phagosomes. The former is physiologically important in cross-presentation in dendritic cells, and the latter prevents the excessive or self-eating phagocytosis in macrophages. Furthermore, the results of our study could contribute to determination of immunological phenotype, even though hyperactivation of macrophages by itself cannot explain the loss of self-recognition and attack of autologous cells that are observed in hemophagocytic syndrome.

In this study, we focused on the role of Rab27a in actin remodeling during the process of phagocytosis. Phagocytosis proceeds as follows: 1) capture of target particles by association between ligands and phagocytic receptors, 2) phagosome formation, 3) internalization, and 4) fusion between lysosomes and phagosomes. First, we found that knockdown of Rab27a increases phagocytic activity, especially during engulfment (Fig. 2, *A* and *B*). In other words, Rab27a negatively regulates phagocytosis during the process of pathogen internalization. We then assessed the role of Rab27a in the process from phagosome formation to internalization using Rab27a knockdown cells. The importance of actin remodeling during the process of phagocytosis has been reported previously (6, 20). The rapid collapse of the actin coat around phagosomes creates a force that leads to internalization of the target particles (7). In fact, we confirmed that pretreatment with the actin-stabilizing agent jasplakinolide clearly inhibits complement-mediated phagocytosis in macrophage-like differentiated HL-60 cells (percentage of the cells that incorporated C3bi-opsonized zymosan was 25 $\pm$ 1.5% of control cells).

In this study, we showed that Rab27a delays the collapse of F-actin around phagosomes via suppression of Coronin 1A accumulation at these sites and prolongs the entire process of phagocytosis (Figs. 3 and 5, *A* and *B*). What is the significance of this delay in internalization? One possibility is that prolonged actin coating gives an opportunity to and a platform for macrophages to recognize the pathogen via known or unknown self-recognition receptors such as the CD47 receptor Signal Regulatory Protein Alpha (SIRPα) (21, 22). Whatever the cause, the mechanism by which Coronin 1A enhances phagocytosis by inducing the rapid collapse of the actin coat might explain the mechanism of non-Griscelli syndrome (type 2), *i.e.* non-hereditary hemophagocytic syndrome.

The critical role of Coronin 1A in actin cup formation during phagocytosis downstream of protein kinase C has been evaluated in a previous report (16). Moreover, it has been reported that a Coronin family protein, Coronin 3, acts as a Rab27a effector molecule in the insulin secretion system (23).

A recent study by Kimura *et al.* (24) demonstrates reduced membrane localization of Coronin 3 in Rab27a knockdown cells and that Coronin 3 associates with GDP-Rab27a. However, we could not detect increased accumulation of Rab27a-T23N only by transfection at the resting stage (before phagocytosis; data not shown), but rescue of Rab27a knockdown cells by Rab27a-T23N clearly promoted the accumulation of Coronin 1A around phagosomes with various colocalization patterns of Rab27a and Coronin 1A on phagosome membranes (supplemental Fig. S1). However, focusing only on colocalization, we observed colocalization of Rab27a and Coronin 1A in the early phase of phagosome formation, even in the case of rescue by wild-type Rab27a (Fig. 5*D*, *left*). Our data indicate that rescue of Rab27a knockdown cells by Rab27a-T23N promotes the serial process of accumulation and dissociation of Coronin 1A on phagosome membranes. The study is the first to propose the hypothesis that Coronin 1A is an effector molecule of Rab27a during phagocytosis. Furthermore, rescue expression of Rab27a-Q78L (GTP-bound form), but not Rab27a-T23N (GDP-bound form), in Rab27a knockdown cells completely abrogated both elevated phagocytosis and increased accumulation of Coronin 1A around phagosomes induced by Rab27a knockdown (Fig. 5*D*).

Hence, we can raise some possibilities about the relation between Rab27a and Coronin 1A as follows: 1) GTP-Rab27a inhibits Coronin 1A function; 2) GDP-Rab27a promotes Coronin 1A function; 3) switching from GTP-Rab27a to GDP-Rab27a releases the inhibition of Coronin 1A function; and 4) Rab27a-T23N exerts a dominant-negative effect on the small amount of wild-type Rab27a remaining in Rab27a knockdown cells, and wild-type Rab27a cannot function. Jayachandran *et al.* (25) reported that the absence of Coronin 1 in J774 macrophages using siRNA does not affect phagocytosis. In contrast, our results showed that Coronin 1A promotes and accelerates phagocytosis, and such a function is regulated by Rab27a. In addition, transfection of Coronin 1A shRNA clearly inhibited the disassembly of F-actin-encapsulating phagosomes and led to a delayed engulfment of particles in macrophage-like differentiated HL-60 cells (supplemental Fig. S2). There seemed to be some differences in cell types and in assay conditions. Further studies are necessary to identify the mechanism by which Rab27a regulates Coronin 1A during the process of actin remodeling during phagocytosis. In conclusion, we have investigated whether Rab27a plays a direct role in the process of phagocytosis, and we have shown that Rab27a negatively regulates phagocytosis by prolongation of the actin-coating stage via suppression of Coronin 1A accumulation at these sites.

REFERENCES

1. Stenmark, H. (2009) *Nat. Rev. Mol. Cell Biol.* **10,** 513–525
2. Ostrowski, M., Carmo, N. B., Krumeich, S., Fanget, I., Raposo, G., Savina, A., Moita, C. F., Schauer, K., Hume, A. N., Freitas, R. P., Goud, B., Benaroch, P., Hacohen, N., Fukuda, M., Desnos, C., Seabra, M. C., Darchen, F., Amigorena, S., Moita, L. F., and Thery, C. (2010) *Nat. Cell Biol.* **12,** 19–30; sup pp. 1–13
3. Kuroda, T. S., and Fukuda, M. (2004) *Nat. Cell Biol.* **6,** 1195–1203
4. Ménasché, G., Pastural, E., Feldmann, J., Certain, S., Ersoy, F., Dupuis, S., Wulffraat, N., Bianchi, D., Fischer, A., Le Deist, F., and de Saint Basile, G. (2000) *Nat. Genet.* **25,** 173–176
5. Ménager, M. M., Ménasché, G., Romao, M., Knapnougel, P., Ho, C. H., Garfa, M., Raposo, G., Feldmann, J., Fischer, A., and de Saint Basile, G. (2007) *Nat. Immunol.* **8,** 257–267

6. Swanson, J. A. (2008) *Nat. Rev. Mol. Cell Biol.* **9,** 639–649
7. Scott, C. C., Dobson, W., Botelho, R. J., Coady-Osberg, N., Chavrier, P., Knecht, D. A., Heath, C., Stahl, P., and Grinstein, S. (2005) *J. Cell Biol.* **169,** 139–149
8. Mao, Y. S., Yamaga, M., Zhu, X., Wei, Y., Sun, H. Q., Wang, J., Yun, M., Wang, Y., Di Paolo, G., Bennett, M., Mellman, I., Abrams, C. S., De Camilli, P., Lu, C. Y., and Yin, H. L. (2009) *J. Cell Biol.* **184,** 281–296
9. Fairn, G. D., Ogata, K., Botelho, R. J., Stahl, P. D., Anderson, R. A., De Camilli, P., Meyer, T., Wodak, S., and Grinstein, S. (2009) *J. Cell Biol.* **187,** 701–714
10. Jancic, C., Savina, A., Wasmeier, C., Tolmachova, T., El-Benna, J., Dang, P. M., Pascolo, S., Gougerot-Pocidalo, M. A., Raposo, G., Seabra, M. C., and Amigorena, S. (2007) *Nat. Cell Biol.* **9,** 367–378
11. Fukuda, M. (2002) *J. Biol. Chem.* **277,** 40118–40124
12. Fukuda, M. (2005) *J. Biochem.* **137,** 9–16
13. Chavas, L. M., Ihara, K., Kawasaki, M., Torii, S., Uejima, T., Kato, R., Izumi, T., and Wakatsuki, S. (2008) *Structure* **16,** 1468–1477
14. Kukimoto-Niino, M., Sakamoto, A., Kanno, E., Hanawa-Suetsugu, K., Terada, T., Shirouzu, M., Fukuda, M., and Yokoyama, S. (2008) *Structure* **16,** 1478–1490
15. Yan, M., Collins, R. F., Grinstein, S., and Trimble, W. S. (2005) *Mol. Biol. Cell* **16,** 3077–3087
16. Oku, T., Kaneko, Y., Murofushi, K., Seyama, Y., Toyoshima, S., and Tsuji, T. (2008) *J. Biol. Chem.* **283,** 28918–28925
17. Tsujita, K., Itoh, T., Kondo, A., Oyama, M., Kozuka-Hata, H., Irino, Y., Hasegawa, J., and Takenawa, T. (2010) *J. Biol. Chem.* **285,** 6781–6789
18. Shi, Y., Tohyama, Y., Kadono, T., He, J., Miah, S. M., Hazama, R., Tanaka, C., Tohyama, K., and Yamamura, H. (2006) *Blood* **107,** 4554–4562
19. Katagiri, K., Katagiri, T., Koyama, Y., Morikawa, M., Yamamoto, T., and Yoshida, T. (1991) *J. Immunol.* **146,** 701–707
20. Liebl, D., and Griffiths, G. (2009) *J. Cell Sci.* **122,** 2935–2945
21. Majeti, R., Chao, M. P., Alizadeh, A. A., Pang, W. W., Jaiswal, S., Gibbs, K. D., Jr., van Rooijen, N., and Weissman, I. L. (2009) *Cell* **138,** 286–299
22. Jaiswal, S., Jamieson, C. H., Pang, W. W., Park, C. Y., Chao, M. P., Majeti, R., Traver, D., van Rooijen, N., and Weissman, I. L. (2009) *Cell* **138,** 271–285
23. Kimura, T., Kaneko, Y., Yamada, S., Ishihara, H., Senda, T., Iwamatsu, A., and Niki, I. (2008) *J. Cell Sci.* **121,** 3092–3098
24. Kimura, T., Taniguchi, S., Toya, K., and Niki, I. (2010) *Biochem. Biophys. Res. Commun.* **395,** 318–323
25. Jayachandran, R., Gatfield, J., Massner, J., Albrecht, I., Zanolari, B., and Pieters, J. (2008) *Mol. Biol. Cell* **19,** 1241–1251